Plant roots steer resilience to perturbation of river floodplains

Plant roots steer resilience to perturbation of river floodplains

Valentina Bau'[1], Alistair G.L. Borthwick [1,2], Paolo Perona[1,3,4]

[1]Institute for Infrastructure and Environment, The University of Edinburgh, Edinburgh EH9 3FG, UK
[2]School of Engineering, Computing and Mathematics, University of Plymouth, Plymouth PL4 8AA, UK
[3]Ecological Engineering Laboratory (ECOL), Institute of Environmental Sciences and Technology (IIE), ENAC Faculty, Ecole Politechnique Federale del Lausanne (EPFL), Lausanne, Switzerland
[4]HOLINGER AG, Urban drainage and hydraulic engineering, Kasthoferstrasse 23, CH-3000 Bern, Switzerland

Key Points:

- We develop a mechanistic model for river floodplain equilibrium states and their response to changing flow regime
- Temporal irreversibility to reversible conditions is shown to originate from plant root adaptation to the new regime
- We use a worldwide common example of water impoundment to quantify long-term floodplain dynamics.

Corresponding author: Valentina Bau', v.bau@ed.ac.uk, valentina.bau.3@gmail.com

Abstract

Freshwater ecosystems along river floodplains host among the greatest biodiversity on Earth and are known to respond to anthropic pressure. For water impounded systems, resilience to changes in the natural flow regime is believed to be bi-directional. Whether such resilience prevents the system from returning to pristine conditions after the flow regime changes reverse is as yet unclear, though widely documented. In this work we show that temporal irreversibility of river floodplains to recover their status may be explained by the dynamics of riparian water-tolerant plant roots. Our model is a quantitative tool that will benefit scientists and practitioners in predicting the impact of changing flow regimes on long-term river floodplain dynamics.

Plain Language Summary

Catchment impoundment and the withdrawal of flowing water from mountain torrents and rivers for human needs are practices that modify the mean discharge and variability of natural streams. The long-term impact includes changes to floodplain morphology and the compositions of terrestrial and aquatic biodiversity. Vegetation encroachment is then widely observed on floodplains where water is not a limiting factor for plants to grow. The extent to which such alterations are reversible is an important object of this study, and has important implications for water management strategies when hydraulic structures reach the end of either their physical life or their economic benefit. We develop a comprehensive theoretical model that reveals the important role of plant roots in these processes. The model is applied to impoundment of the River Maggia in Switzerland. It is found that natural conditions before dam construction might not be fully restored by simply removing the dam. Our approach offers an important step towards improving natural water management schemes and optimal dam regulation strategies in the face of human and climatic hydrological changes.

1 Introduction

River impoundment is a water management practice used worldwide that primarily affects the river natural flow regime. Often exacerbated by a lack of sustainable management actions, alterations to the flow regime provide a major source of anthropic pressure on freshwater ecosystems (Stella & Bendix, 2019). The process first affects the river-

ine geomorphic asset and may later change the ecologic integrity of related biota communities (Bunn & Arthington, 2002; Poff et al., 1997; Rosenberg et al., 2000; Tullos et al., 2004). In the long term, floodplain and riparian zones gradually lose their functional, societal, and economic values (E. Wohl et al., 2005). About 48% of all world river systems are regulated nowadays, and this proportion is forecast to rise to 93% by 2030 (Grill et al., 2015). Urgency measures have now become an inherent part of the biodiversity strategy program (EC, 2020). Commencement of dam operations typically causes downward shifts in mean streamflow and corresponding river stages, the disappearance of moderate flooding events, and sediment flow interruption. When sediment inflow is interrupted by a dam, the altered sediment-carrying capacity of the river leads to incision and entrenchment of the channel, thus promoting disconnection between the channel and the floodplain (E. E. Wohl, 2004). River hydrograph attributes (Trush et al., 2000) are also important in controlling the development of juvenile vegetation (Kui et al., 2017; Stella et al., 2006). Following a downward shift in water table perhaps enhanced by channel incision, plant roots may travel deeper in soil in order to track soil moisture even at higher elevation differences (Smith, 2007; Pasquale et al., 2012). Such an hydrotropic response also reshapes the vertical root density distribution of riparian plants (Gorla et al., 2015). Hence, a frequently observed transient floodplain response to hydrologic regime shift begins with intense riparian vegetation establishment and encroachment causing river channel narrowing (Choi et al., 2005; Gordon & Meentemeyer, 2006; Allred & Schmidt, 1999; Molnar et al., 2008; Stella et al., 2003). From a dynamical system perspective, such eco-geomorphic transformations occur as a 'transient phase' that may last for decades (Petts, 1987), before the riverine ecosystem adjusts to a new dynamic equilibrium (Petts, 1984). According to Petts (1987), the 'transient phase' depends on several factors including channel type, mobility of sediment and channel boundaries, biota species adaptation, etc. The degree of reversibility of the transformation processes upon restoring pristine hydrologic conditions is largely unknown (Molnar et al., 2008; Perona, Camporeale, et al., 2009; Tullos et al., 2009).

Ecosystem shifts following perturbation have often been ascribed to catastrophe-like dynamics. A tipping point (i.e., bifurcation) towards new stable equilibria occurs when some key system parameter acting as the system driver reaches a critical value (Scheffer et al., 2001). A key feature of such catastrophic transitions is their hysteretic behaviour and irreversibility when the system driver conditions are reversed. It is therefore tempt-

ing to draw ideas from catastrophe theory to explain the effect of river impoundment on freshwater ecosystems. However, May (1977) observed that ecosystem dynamics may possess multiple stable equilibrium points and Zahler and Sussmann (1977) pointed out that irreversibility may not necessarily be a consequence of catastrophic transitions. Our present work expands on this idea.

Ecomorphodynamics systems theory has elegantly explained how different fluvial styles can be the result of a triad process involving water, sediment and vegetation dynamics (Bärenbold et al., 2016; Bertagni et al., 2018; Caponi & Siviglia, 2018). A means by which to unravel information and thus quantify the extent and reversibility of floodplain changes to hydrological perturbations is offered by modelling the response of riparian plants and their root systems to perturbation. The analytical tractability of spatial mathematical models inevitably requires simplification even without explicitly considering the dynamics of root adaptation (Bertagni et al., 2018; Caponi et al., 2019). However, further steps in this direction can be achieved by focusing on point rather than distributed spatial resolution. This is sufficient to show how resistance to uprooting responds to a changing flow regime and to what extent the process is reversible.

In this work, we develop a comprehensive model that accounts for the evolution of plant uprooting by flow after impoundment, and describes the (stable) equilibrium states of the floodplain system at a point. The complex dynamics of river floodplain response to perturbation are thus reduced to that of a dynamical system represented by a suitable state variable. In particular, we investigate the existence of novel stable equilibrium states for perturbed riverine corridors and discuss their possible irreversibility. The model is applied to a typical example of dam impoundment, which is common worldwide and is known to lead to intense riparian vegetation encroachment with consequent river narrowing (Molnar et al., 2008; Perona, Molnar, et al., 2009).

2 Riparian processes and model formulation

Figure 1a indicates how roots of phreatophytic vegetation tend to adapt to water table fluctuations. At high elevations above the phreatic surface, the plant root biomass distribution locates preferentially deep into the soil. Conversely, at lower elevations close to the phreatic surface the root biomass distribution is shallow and highly developed near the soil surface (Tron et al., 2015). Therefore, a vertical (down)shift in the water table

may not necessarily hinder the growth of phreatophytic species, but instead affect their rooting depth and vertical distribution (Gorla et al., 2015). In turn, the anchorage depth of roots influences the ability of a plant to withstand erosion processes and its survival probability to uprooting by flow (Docker & Hubble, 2008; Pasquale et al., 2014; Simon & Collison, 2002). Here, we combine stochastic and deterministic approaches of riparian vegetation dynamics into a comprehensive and almost entirely analytical framework. Accordingly, we use the probability of plant uprooting by flow, P_τ as a proxy variable to represent the statistical state of the floodplain at a given time. Hence, it is implicitly assumed that vegetation mortality is solely caused by flow-induced uprooting; other mechanisms such as plant burial have not been considered because their effect may also favor vegetation survival (Kui & Stella, 2016; Politti et al., 2018). Plant uprooting probability depends on: plant elevation with respect to riverbed elevation; the representative mean flow erosion event at the riverbed elevation; and the critical scour depth for the plant (Perona & Crouzy, 2018). Both latter quantities depend on the statistical properties of the river discharge (and water levels), which obviously differ between pre- and post-impoundment periods. We now proceed toward assembling all processes in the model.

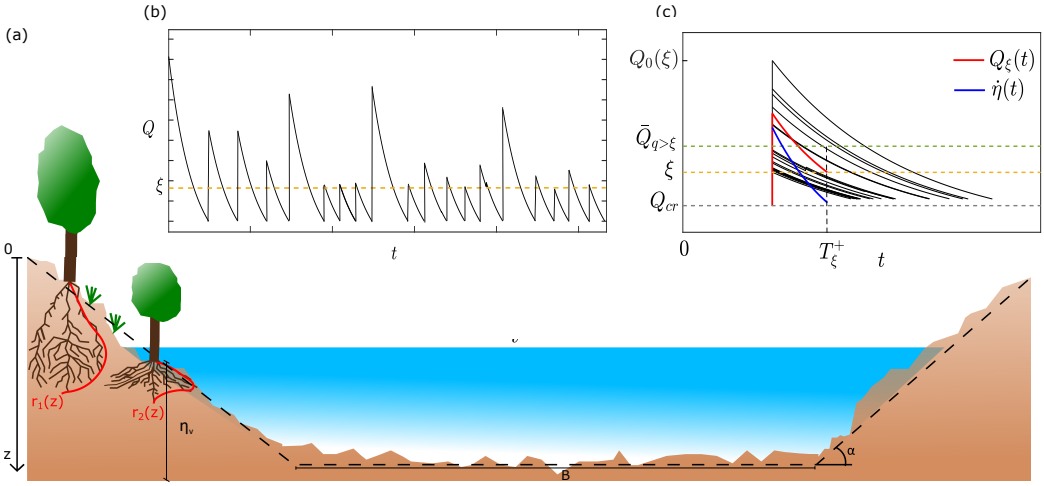

Figure 1. Sketch of the modeling framework. a) Illustration of the river section and its trapezoidal idealization (black dashed line) with riverbanks inclined at angle α with respect to the riverbed. The two plants located on the riverbanks display different root biomass profiles, which may be represented analytically as $r_1(z)$ and $r_2(z)$ where z is the depth below the soil surface using the model proposed by Tron et al. (2014). b) Synthetic hydrologic signal of the flow discharge (CPP); ξ demarks the prescribed threshold when implementing Peak Over Threshold Theory. c) Sequence of events that lie above the threshold ξ. The statistical average of all the events is the mean reference event (red line). The blue line represents the bed erosion rate (modified from Calvani et al. (2019)).

2.1 Probability distribution of time to uprooting

Perona and Crouzy (2018) modelled plant uprooting by flow as a result of stochastic erosion dynamics requiring a time interval T to scour the bed to the critical depth leading to plant collapse. They obtained the following analytical expression for the probability density function (pdf) of the elapsed time T to uprooting p_τ for flow erosion events of generic shape and plant critical rooting depth:

$$p_\tau(T) = \frac{L_e}{2\sqrt{\pi G(T)^3}} e^{\left(-\frac{(L_e - V(T))^2}{4G(T)}\right)} \left[\frac{g_t(T)}{2} + e^{\left(\frac{(L_e + V(T))^2}{4G(T)}\right)} W(T)\right] \tag{1}$$

where $g_t(T)$ describes the noise affecting the erosion process at time $t = T$, $G(T) = \frac{1}{2}\int_0^T g_t(\tau)d\tau$, $V(T) = \int_0^T \dot{\eta}(\tau)d\tau$, $W(T) = \sqrt{\pi}\mathrm{Erfc}\left[\frac{L_e + V(T)}{2\sqrt{G(T)}}\right]\left(\dot{\eta}(T)\sqrt{G(T)} - \frac{g_t(T)}{2}\frac{V(T)}{\sqrt{G(T)}}\right)$, and τ is the dummy variable of integration. L_e is the scouring depth that determines uprooting, and $\dot{\eta}(t)$ is the erosion rate event corresponding to the plant elevation. Values of L_e and $\dot{\eta}(t)$ are assessed in sections 2.4 and 2.5. The following expression for g_t is obtained assuming that erosion may be represented by a Ornstein-Uhlenbeck stochastic flow process, in which the flow velocity profile is logarithmic and fluctuations acting on sediment particles follow Einstein's diffusion theory (for more details, see the mathematical derivation of equation (8) in the Supporting Information (SI)):

$$g_t = 8.5 D_{50} u_* \tag{2}$$

where D_{50} is the median grain size of the sediment, and u_* is the shear velocity.

2.2 Water discharge and groundwater level dynamics

Variability in both the water discharge and groundwater levels is addressed using a Compound Poisson process (CPP) (Ridolfi et al., 2011), comprising white shot-noise random positive pulses followed by deterministic decays (Figure 1b). Hence, the pdf of flow discharge is given by:

$$p(Q) = \frac{\gamma_d^{-\beta_d}}{\Gamma[\beta_d]} e^{-Q/\gamma_d} Q^{(\beta_d - 1)}, \tag{3}$$

where Q is the flow rate, $\Gamma[\cdot]$ is the Gamma function (Abramowitz & Stegun, 1948), γ_d is the mean amplitude of the pulses and β_d is the product between the mean frequency of the jumps, λ_d, and the deterministic exponential decay rate, τ_d (see, also SI). Next, we use normal flow conditions to obtain the corresponding water level at each cross sec-

tion of interest. Likewise, we assume that water stage follows a CPP with parameters γ_l and β_l that are fitted to the empirical pdf of water level (see also SI) and synchronously drive the dynamics of the phreatic water table in the soil Tron et al. (2014).

2.3 Grain size distribution

The bed erosion rate and root profile require input values for D_{50}, D_{10}, and D_{90}, which are respectively the median, the tenth, and the ninetieth percentiles of the sediment size distribution. To account for the sediment retention capacity of the dam and the reduction in bed mobility downstream, a shift in sediment size between pre- and post-dam periods was included in the modelling framework (Yang et al., 2014). Thus, we did not explicitly model sediment sorting and bed armoring processes; instead, we empirically modelled sediment size increase in the post-dam period.

2.4 Root profile and scour depth

According to Perona and Crouzy (2018), the probability of uprooting depends on the scouring depth, $L_e = L_0 - L_c$, which is the difference between the effective rooting length and the critical rooting length leading to uprooting. We obtain L_e by combining the model proposed by Tron et al. (2014) for the vertical root profile, $r(z)$, where z is distance below the riverbed level, with that by Bau' et al. (2019) for the critical rooting length, L_c. As shown in the SI, L_e can be obtained by solving the following integral:

$$L_{e,t} = a_m \int_0^{L_e} r(z)dz \tag{4}$$

where $L_{e,t}$ indicates the flow-exposed total rooting length due to scour, and a_m is a proportionality constant that links $L_{e,t}$ to its corresponding root biomass, here expressed through the integral of $r(z)$. The mathematical derivation of equation 4 and further details of the parameters $L_{e,t}$ and a_m are given in the Supporting Information.

2.5 Reference mean event and bed erosion rate

Estimation of the probability of uprooting requires knowledge of the temporal evolution of a reference mean erosion event above a given threshold. For simplicity, we assume the threshold ξ for onset erosion coincides with the discharge that just starts to inundate the plant at its elevation, η_v (see Figure 1). Thereby, erosion (and therefore

potential uprooting) at a given location can only occur for flood events whose stage reaches or exceeds the bed elevation at that location, i.e. for values that lie above ξ. To determine the reference flow event we therefore use the mean of all such events obtained analytically from Calvani et al. (2019),

$$Q_\xi(t) = Q_0(\xi)e^{-t/\tau_1} \tag{5}$$

where Q_0 is the mean of all peak events exceeding the threshold ξ, and τ_1 is the integral temporal scale of the reference mean event. The reference mean event (red line in Figure 1c) ceases at T_ξ^+, which is the up-crossing period of the signal.

From the reference mean discharge event, we then obtain the reference bed erosion event associated with the reference flow event as per Calvani et al. (2019):

$$\dot{\eta}(t) = \frac{1}{(1-\lambda_g)\Delta X}\alpha_{BL}\left(\frac{\left(\frac{Q_\xi(t)}{A\sqrt{S}K_s}\right)^{3/2}S}{D_{50}(\frac{\rho_g-\rho_w}{\rho_w})} - \tau_{cr}^*\right)^b D_{50}\sqrt{\frac{\rho_g-\rho_w}{\rho_w}gD_{50}}, \tag{6}$$

where λ_g is the sediment porosity, ΔX is the erosion length scale, α_{BL} is the coefficient in the bed-load transport formula, A is the wet cross-sectional area of the river, K_s the Strickler coefficient of the sediment, g the acceleration due to gravity, ρ_g is the density of the sediment, τ_{cr}^* is the critical Shields parameter, and b is the exponent in the sediment transport formula. Equation 6 applies to a point in a generic river section and has been obtained by combining the 1D-Exner equation for conditions of net bed erosion (e.g. negligible sediment inflow at the point) with a Meyer-Peter and Müller type sediment transport relationship. The mean erosion event is depicted by the blue line in Figure 1c.

3 Results from model application to an actual case study

The model is applied to the case study of the river Maggia, as it flows through the Valle Maggia in Tessin, Switzerland. After impoundment by dams commenced in 1953, the river discharge experienced a severe hydrologic shift, which triggered vegetation encroachment and gradual channel narrowing (Ruf et al., 2007; Molnar et al., 2008; Perona, Molnar, et al., 2009). The SI provides a description of relevant data and the calculation of all model parameters. Note that dam impoundment led to a decrease in τ_d (from 3.31 to 1.60 d) and λ_d (from 0.22 to 0.05 d^{-1}), and to an increase in γ_d (from 23 to 50 m^3/s). The product $\gamma_d\lambda_d\tau_d$ gives the mean flow discharge of the CPP signal μ_d.

The values obtained for μ_d coincide with mean values of the actual hydrographs, which are 16.5 m^3/s and 4 m^3/s for the periods 1933-1953 and 1954-2007, respectively. A table listing values assigned to the parameters in the equations presented in Section 2 has been included in the SI. Apart from data retrieved from the literature and previous studies of the Maggia Valley, values of several parameters (related to plant properties and geometry) had to be estimated owing to lack of information. The model satisfactorily represents the expected behaviour of the hydrograph, as shown in Figure 2b. During the post-dam period only the highest river discharge peaks characterise the hydrograph, unlike for the pre-dam period. These peaks correspond to a CPP having higher intensity, lower frequency, and lower temporal correlation. The probability of uprooting P_τ was calculated by numerically integrating Eq.(1) over the duration of the erosion event, and plotting the result as a function of increasing ΔH (i.e. the difference between plant riverbed elevation and mean water stage for increasing hydrograph (down)shifts). Hence, ΔH represents the driver in terms of hypothetical hydrologic shift severity caused by impoundment.

Figure 2a shows the location of the stable statistical equilibrium states (blue points) of the river floodplain state (represented by P_τ) for increasing ΔH. Pre-dam conditions are represented by the point P1, indicating that plants had more than 90% probability of being uprooted by the reference mean erosion event of the pre-dam hydrograph. The colour-rendered aerial photographs (1933, 1944, colour legend in Figure caption) show the floodplain morphology before dams started to operate. Dam operation produced a vertical downshift in mean discharge (and water stages) (see Figure 2b), i.e. a sudden increase of ΔH brought the system to the 'out-of-equilibrium' point P2, where plants still had the root architecture of pristine conditions, but were suddenly exposed to post-dam erosion event scenarios. In this case, the probability of uprooting remained high and the image from 1962 shows a floodplain almost without water but with a high braiding index. In the post-dam period (point P2), plant roots started to adapt to the lower water table conditions by deepening root biomass and consequentially reducing the probability of uprooting. This process was gradual, and it took several years for the floodplain system to reach the point P3 (see images 1995 and 2006), which represents the new stable equilibrium for the post-dam hydrological conditions. The same reasoning can be repeated for hypothetical milder shifts of the driver, i.e. ΔH, thus obtaining the blue sequence of stable equilibrium states joining points P1 and P3. The process of discon-

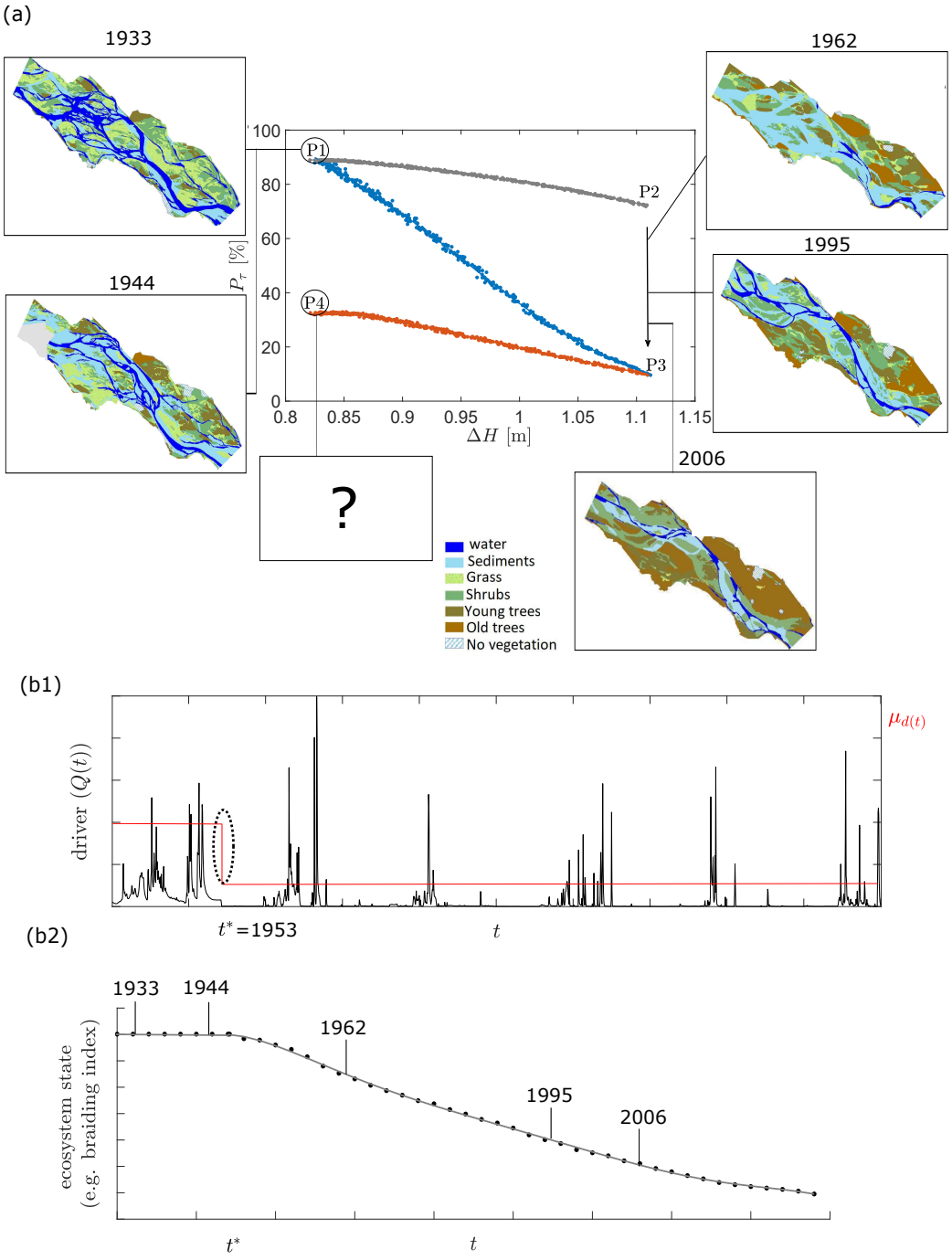

Figure 2. a) Uprooting probability, P_τ, plotted against ΔH, for plant elevation, $\eta_v = 1.2$ m. The insets show the morphological evolution of the river floodplain in 1933, 1944, 1962, 1995, and 2006. b1) Time series of the driver (flow discharge). Note that the value represented for the mean flow rate, μ_d, is offset for illustrative purposes. b2) Time series of the ecosystem state (braiding index). The years illustrated are intended to recall the evolution of the spatial distribution shown in the subplots in Figure a).

nection between the floodplain and the main channel due to channel incision was not considered here and might lead to two opposite scenarios. For vegetation species able to track the lowering of the water table, their root biomass may deepen further in soil and the probability of plant uprooting by flooding events would further decrease. On the contrary, vegetation species with low adaptation capability would possibly die and slowly lead to a non-vegetated system, which is not object of this study. Hence, the first scenario necessarily implies that the value of P_τ in the post-dam period may change when considering the ability of different plant species to adapt to extreme and sudden drought conditions. This indirectly explains plant speciation and invasion by species that tolerate and/or favor the new conditions.

For a system in state P3, hypothetical dam removal and return to the natural flow regime would imply a sudden reduction in ΔH to its original value. The system would thus jump to the point P4. Notwithstanding that flow erosion events at point P4 are more frequent and have the same erosion capacity as those at point P1, the deep root system prevents recovery of the original probability of uprooting, thus explaining the tendency of the floodplain to maintain its current narrow morphology.

Given that the model describes only the stable equilibrium points of the system, it is nevertheless instructive to consider the expected dynamics throughout the time domain (Figure 2b2). Up to time t^* the system state is at point P1. The state then jumps from P2 to P3 at $t = t^*$, following the hydrologic shift of the driver. From point P2 onward, the probability of uprooting declines, presenting a temporal picture as to how the system states transition from state P2 to P3. The time lapse over which the curve decreases represents the 'relaxation time' of the system (in other words, the time required by the ecosystem state to adapt to the new equilibrium). A sensitivity analysis concerning the most relevant input parameters is enclosed in the Supporting Information. An important result of the sensitivity analysis emerges when the grain size distribution is maintained constant between pre- and post-dam periods. This preserves the retention capacity of the soil and hence the zone favorable for root growth. For a plant elevation equal to 1.2 m, this results in a value of uprooting probability at the stable equilibrium point P3 that is four times higher than that in Figure 2a). Maintaining sediment continuity in the post-dam period would thus help vegetation control.

4 Discussions, implications and conclusions

The proposed model has shed light on the type of transitions and temporal irreversibility that potentially affect a river floodplain following hydrological regime shifts. Figure 3 summarizes this process. The curve between P1 and P3 represents the statistical (stable) equilibrium points at which the probability of uprooting follows the progressive adjustment of the root system to the imposed hydrological conditions. In other words, this curve represents a succession of steady states resulting from a quasi-static change in hydrologic conditions. Hence, this segment of the curve can be compared to quasi-static transformations occurring in thermodynamics, where the system always remains at equilibrium. The inability of the system to recover its pristine conditions, e.g. such as returning from point P_4 to point P_1 may be ascribed to the development of deep roots as they track the changing water table conditions. However, the model does not explain the dynamical origin of such irreversibility, causing P_4 to also be a stable equilibrium point. This picture appears plausible for water tolerant plants, such as riparian plants. Their roots may tolerate long periods under soil saturated conditions. Hence, in returning to the original natural flow regime, new deep roots would no longer form, and existing roots might not die off but instead persist in the soil for the entire life time of the plant. Conversely, plant species not tolerating submersed conditions would simply die off and be replaced by others, thus delaying the return to pristine conditions (temporary irreversibility) for which P_4 would be out-of-equilibrium.

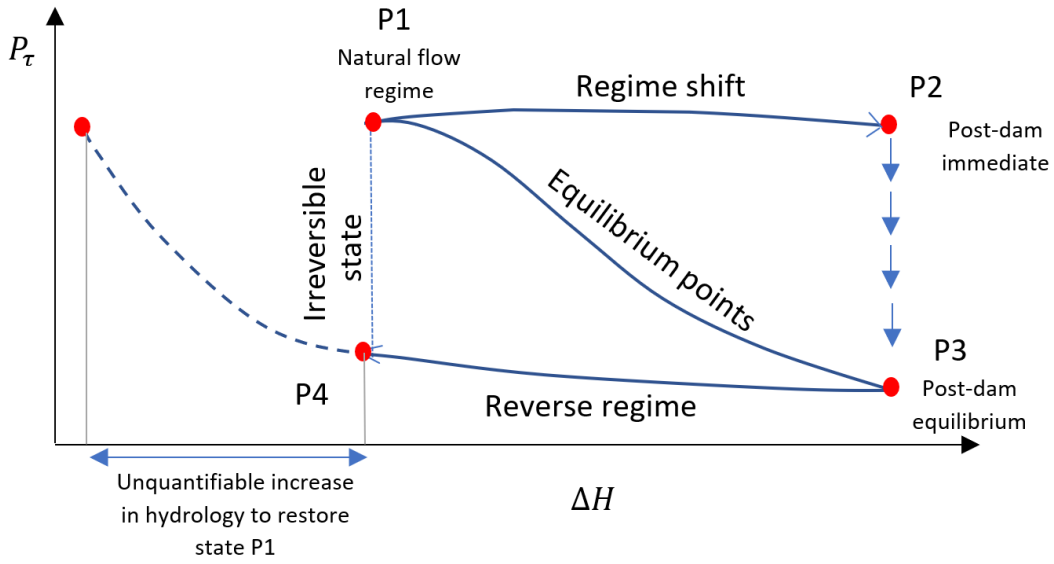

Figure 3. Detailed sketch of the different regime transitions of the ecosystem state.

Similar dynamics have also been documented in the literature, but have never been modeled quantitatively. For instance, Auble et al. (2007) found that vegetation recovery following removal of a dam is complex and does not follow a reversal response, leading to the necessity for river restoration intervention. Hence, if dams were to be removed, vegetation coverage and community would not be much affected, leading to a long-term impact on vegetation succession, especially in systems with low sediment transport (Hobbs et al., 2009). The removal of invasive species that often colonise terraces and benches of dammed rivers is extremely complex (Foley et al., 2017), making the process of reintroduction of native species difficult to achieve (Orr & Stanley, 2006; Tullos et al., 2016). For instance, the vegetation response following dam removal on the Souhegan River in Merrimack (USA) merely consisted of changes to certain herbaceous plants growing closest to the river channel and in the off-channel wetland (Lisius et al., 2018). Furthermore, intensive establishment of mature vegetation during the post-dam period would increase riverbank stability, thus also making it difficult for the river morphology to re-establish its natural pattern (Shafroth et al., 2002). This was also documented by Pearson et al. (2011), who stated that the process of morphological recovery of the Souhegan River has been influenced by the segmentation of alluvial and non-alluvial sections that had been marked by establishment of vegetation on the channel banks during impoundment. Again this, in some measure, is satisfactorily explained by the reduced probability of uprooting by flow caused by plant root hydrotropic response. Shafroth et al. (2002) also suggested that the persistent occurrence of transient phases after dam construction has a determinant impact on the life duration of mature vegetation (e.g. forest), which could persist for even more than a century. In practice, mature vegetation cannot easily be removed by flow erosion processes and return to point P1 may only happen for erosion events of very large return periods or by mechanical action (e.g., restoration). At this point we speculate that a reasonable model representing such an out-of-equilibrium system dynamics could have the form

$$\frac{dP_\tau}{dt} = f_1(P_\tau) - f_2(1 - P_\tau), \tag{7}$$

where $f_1(P_\tau)$ represents the positive tendency of the system to reduce the root biomass, which would facilitate uprooting. Conversely, $f_2(1-P_\tau)$, represents the tendency of the system to modify and increase the root biomass in order to decrease the uprooting probability, thus favoring plant survival. Clearly, as P_τ depends on the parameter ΔH, then

the (likely nonlinear) form of f_1 and f_2 should be such that the equation $f_1(P_\tau) - f_2(1 - P_\tau) = 0$ describes all the equilibrium points (stable and unstable). The fact that the stable equilibrium points of our model joining P_1 and P_3 all lie on a continuous curve suggests that non-reversibility may be ascribed to the presence of other stable equilibrium points (e.g., P_4) for the general ecosystem dynamics (May, 1977) rather than to a catastrophic-like mechanism. Such multiple points would represent the capability of water tolerant plants to develop and maintain alive deep roots that tolerate anoxia when conditions are reversed.

Our sensitivity analysis (see SI) has also shown that the effective particle size of fine sediment plays an important role in uprooting probability. Hence, replenishment of fine sediment could offer a potential way of maintaining the uprooting percentages for post-dam conditions at levels closer to those for pre-dam conditions. Such a goal could be achieved for instance by inducing artificial floods, a well-established technique used to reduce river morphological changes after dam impoundment. In the present application, artificial flooding should be controlled to ensure that the increase in frequency of peak events would bound the erosion rate so as to hinder river narrowing and incision, and stream-bank erosion (Stähly et al., 2019). This strategy could also be adopted to reduce the accumulation of fine sediment upstream of a dam, whose presence considerably limits the storage capacity of the associated reservoir. The input of fine sediment would not only benefit the shape of the river but also its biodiversity, thus preventing the riparian system from drifting to alternative states (Arheimer et al., 2018). The artificial flooding strategy appears to be promising in terms of effectiveness. This is also confirmed by results obtained by Perona, Camporeale, et al. (2009), who used a lumped model to predict that adding an artificial disturbance each year would lead to increases of 10% in both sediment and water area in the Maggia River reach considered herein.

To conclude, plant root profile can affect riparian ecosystem resilience to pressures such as hydrological alterations and flow erosion processes. Our results suggest that initial state conditions may only be restored after impoundment through the occurrence of an hydrologic event of a much larger return period or by the clearance of riparian vegetation through deforestation and river restoration. This novel combined method can identify and complement dam regulation strategies and promote sustainable solutions to preserve terrestrial and aquatic ecosystems before planetary boundaries are reached (Steffen et al., 2015).

Acknowledgments

No new data has been used for this research. Part of the data used to implement the model is available in the following in-text data citation reference: Ruf (2007). The aerial images illustrated in Figure 2a) can be found online on Mendeley Data (http://dx.doi.org/10.17632/czjwgb9jp8.1).

References

Abramowitz, M., & Stegun, I. A. (1948). *Handbook of mathematical functions with formulas, graphs, and mathematical tables* (Vol. 55). US Government printing office.

Allred, T. M., & Schmidt, J. C. (1999). Channel narrowing by vertical accretion along the Green River near Green River, Utah. *Geological Society of America Bulletin*, *111*(12), 1757–1772.

Arheimer, B., Hjerdt, N., & Lindström, G. (2018). Artificially induced floods to manage forest habitats under climate change. *Frontiers in Environmental Science*, *6*, 102.

Auble, G. T., Shafroth, P. B., Scott, M. L., & Roelle, J. E. (2007). Early vegetation development on an exposed reservoir: implications for dam removal. *Environmental Management*, *39*(6), 806–818.

Bärenbold, F., Crouzy, B., & Perona, P. (2016). Stability analysis of ecomorphodynamic equations. *Water Resources Research*, *52*(2), 1070–1088.

Bau', V., Zen, S., Calvani, G., & Perona, P. (2019). Extracting the critical rooting length in plant uprooting by flow from pullout experiments. *Water Resources Research*.

Bertagni, M. B., Perona, P., & Camporeale, C. (2018). Parametric transitions between bare and vegetated states in water-driven patterns. *Proceedings of the National Academy of Sciences*, *115*(32), 8125–8130.

Bunn, S. E., & Arthington, A. H. (2002). Basic principles and ecological consequences of altered flow regimes for aquatic biodiversity. *Environmental Management*, *30*(4), 492–507.

Calvani, G., Perona, P., Zen, S., Bau', V., & Solari, L. (2019). Return period of vegetation uprooting by flow. *Journal of Hydrology*, *578*, 124103.

Caponi, F., Koch, A., Bertoldi, W., Vetsch, D. F., & Siviglia, A. (2019). When does vegetation establish on gravel bars? Observations and modelling in the Alpine

Rhine river. *Frontiers in Environmental Science*, *7*, 124.

Caponi, F., & Siviglia, A. (2018). Numerical modeling of plant root controls on gravel bed river morphodynamics. *Geophysical Research Letters*, *45*(17), 9013–9023.

Choi, S.-U., Yoon, B., & Woo, H. (2005). Effects of dam-induced flow regime change on downstream river morphology and vegetation cover in the Hwang River, Korea. *River Research and Applications*, *21*(2-3), 315–325.

Docker, B., & Hubble, T. (2008). Quantifying root-reinforcement of river bank soils by four Australian tree species. *Geomorphology*, *100*(3-4), 401–418.

EC. (2020). Communication from the commission to the European parliament, the council, the European economic and social committee and the committee of the regions. *A new skills agenda for Europe. Brussels*.

Edmaier, K., Crouzy, B., Ennos, R., Burlando, P., & Perona, P. (2014). Influence of root characteristics and soil variables on the uprooting mechanics of Avena sativa and Medicago sativa seedlings. *Earth Surface Processes and Landforms*, *39*(10), 1354–1364.

Einstein, A. (1905). Über die von der molekularkinetischen Theorie der Wärme geforderte Bewegung von in ruhenden Flüssigkeiten suspendierten Teilchen. *Annalen der Physik*, *322*(8), 549-560.

Foley, M. M., Bellmore, J., O'Connor, J. E., Duda, J. J., East, A. E., Grant, G., ... others (2017). Dam removal: Listening in. *Water Resources Research*, *53*(7), 5229–5246.

Gordon, E., & Meentemeyer, R. K. (2006). Effects of dam operation and land use on stream channel morphology and riparian vegetation. *Geomorphology*, *82*(3-4), 412–429.

Gorla, L., Signarbieux, C., Turberg, P., Buttler, A., & Perona, P. (2015). Transient response of Salix cuttings to changing water level regimes. *Water Resources Research*, *51*(3), 1758–1774.

Grill, G., Lehner, B., Lumsdon, A. E., MacDonald, G. K., Zarfl, C., & Liermann, C. R. (2015). An index-based framework for assessing patterns and trends in river fragmentation and flow regulation by global dams at multiple scales. *Environmental Research Letters*, *10*(1), 015001.

Hobbs, R. J., Higgs, E., & Harris, J. A. (2009). Novel ecosystems: implications

418 for conservation and restoration. *Trends in Ecology & Evolution*, *24*(11), 599–
419 605.

420 Hrissanthou, V., & Kaffas, K. (2019). *Soil erosion: Rainfall erosivity and risk as-*
421 *sessment*. IntechOpen.

422 Järvelä, J. (2002). Determination of flow resistance of vegetated channel banks
423 and floodplains. In B. . Zech (Ed.), *River flow 2002* (pp. 311–318). Swets &
424 Zeitlinger, Lisse.

425 Kui, L., & Stella, J. C. (2016). Fluvial sediment burial increases mortality of young
426 riparian trees but induces compensatory growth response in survivors. *Forest*
427 *Ecology and Management*, *366*, 32–40.

428 Kui, L., Stella, J. C., Shafroth, P. B., House, P. K., & Wilcox, A. C. (2017). The
429 long-term legacy of geomorphic and riparian vegetation feedbacks on the
430 dammed bill williams river, arizona, usa. *Ecohydrology*, *10*(4), e1839.

431 Leopold, L. B., & Wolman, M. G. (1957). *River channel patterns: braided, meander-*
432 *ing, and straight*. US Government Printing Office.

433 Lisius, G. L., Snyder, N. P., & Collins, M. J. (2018). Vegetation community response
434 to hydrologic and geomorphic changes following dam removal. *River Research*
435 *and Applications*, *34*(4), 317–327.

436 May, R. M. (1977). Thresholds and breakpoints in ecosystems with a multiplicity of
437 stable states. *Nature*, *269*, 471 – 477.

438 Molnar, P., Favre, V., Perona, P., Burlando, P., Randin, C., & Ruf, W. (2008).
439 Floodplain forest dynamics in a hydrologically altered mountain river. *Peck-*
440 *iana*, *5*, 17–24.

441 Orr, C. H., & Stanley, E. H. (2006). Vegetation development and restoration poten-
442 tial of drained reservoirs following dam removal in wisconsin. *River Research*
443 *and Applications*, *22*(3), 281–295.

444 Papanicolaou, A., Diplas, P., Evaggelopoulos, N., & Fotopoulos, S. (2002). Stochas-
445 tic incipient motion criterion for spheres under various bed packing conditions.
446 *Journal of Hydraulic Engineering*, *128*(4), 369–380.

447 Parker, G., Wilcock, P. R., Paola, C., Dietrich, W. E., & Pitlick, J. (2007). Phys-
448 ical basis for quasi-universal relations describing bankfull hydraulic geometry
449 of single-thread gravel bed rivers. *Journal of Geophysical Research: Earth*
450 *Surface*, *112*(F4).

Pasquale, N., Perona, P., Francis, R., & Burlando, P. (2012). Effects of streamflow variability on the vertical root density distribution of willow cutting experiments. *Ecological Engineering*, *40*, 167–172.

Pasquale, N., Perona, P., Francis, R., & Burlando, P. (2014). Above-ground and below-ground Salix dynamics in response to river processes. *Hydrological Processes*, *28*, 5189-5203.

Pearson, A. J., Snyder, N. P., & Collins, M. J. (2011). Rates and processes of channel response to dam removal with a sand-filled impoundment. *Water Resources Research*, *47*(8).

Perona, P., Camporeale, C., Perucca, E., Savina, M., Molnar, P., Burlando, P., & Ridolfi, L. (2009). Modelling river and riparian vegetation interactions and related importance for sustainable ecosystem management. *Aquatic Sciences*, *71*(3), 266.

Perona, P., & Crouzy, B. (2018). Resilience of riverbed vegetation to uprooting by flow. *Proceedings of the Royal Society A: Mathematical, Physical and Engineering Sciences*, *474*(2211), 20170547.

Perona, P., Molnar, P., Savina, M., & Burlando, P. (2009). An observations-based stochastic model for sediment and vegetation dynamics in the floodplain of an Alpine braided river. *Water Resources Research*, *45*, W09418.

Petts, G. E. (1984). *Impounded rivers: perspectives for ecological management.* Wiley.

Petts, G. E. (1987). Time-scales for ecological change in regulated rivers. In *Regulated streams* (pp. 257–266). Springer.

Poff, N. L., Allan, J. D., Bain, M. B., Karr, J. R., Prestegaard, K. L., Richter, B. D., ... Stromberg, J. C. (1997). The natural flow regime. *BioScience*, *47*(11), 769–784.

Politti, E., Bertoldi, W., Gurnell, A., & Henshaw, A. (2018). Feedbacks between the riparian salicaceae and hydrogeomorphic processes: A quantitative review. *Earth-Science Reviews*, *176*, 147–165.

Ridolfi, L., D'Odorico, P., & Laio, F. (2011). *Noise-induced phenomena in the environmental sciences.* Cambridge University Press.

Rodriguez-Iturbe, I., Porporato, A., Ridolfi, L., Isham, V., & Cox, D. (1999). Probabilistic modelling of water balance at a point: the role of climate, soil and

vegetation. *Proc. R. Soc. Lond. A*, *455*, 3789-3805.

Rosenberg, D. M., McCully, P., & Pringle, C. M. (2000). Global-scale environmental effects of hydrological alterations: introduction. *BioScience*, *50*(9), 746–751.

Ruf, W. (2007). *Numerical modelling of distributed river: aquifer coupling in an alpine floodplain* (Ph.D. thesis). ETH Zurich.

Ruf, W., Foglia, L., Perona, P., Molnar, P., Faeh, R., & Burlando, P. (2007). *Modelling the interaction between groundwater and river flow in an active alpine floodplain ecosystem* (Unpublished doctoral dissertation). ETH Zurich.

Scheffer, M., Carpenter, S., Foley, J. A., Folke, C., & Walker, B. (2001). Catastrophic shifts in ecosystems. *Nature*, *413*(6856), 591–596.

Shafroth, P. B., Friedman, J. M., Auble, G. T., Scott, M. L., & Braatne, J. H. (2002). Potential responses of riparian vegetation to dam removal: dam removal generally causes changes to aspects of the physical environment that influence the establishment and growth of riparian vegetation. *BioScience*, *52*(8), 703–712.

Simon, A., & Collison, A. J. (2002). Quantifying the mechanical and hydrologic effects of riparian vegetation on streambank stability. *Earth Surface Processes and Landforms*, *27*(5), 527–546.

Smith, F. A. (2007). *Plant roots. growth, activity and interaction with soils.* Oxford University Press.

Stähly, S., Franca, M. J., Robinson, C. T., & Schleiss, A. J. (2019). Sediment replenishment combined with an artificial flood improves river habitats downstream of a dam. *Scientific Reports*, *9*(1), 1–8.

Steffen, W., Richardson, K., Rockström, J., Cornell, S. E., Fetzer, I., Bennett, E. M., ... others (2015). Planetary boundaries: Guiding human development on a changing planet. *Science*, *347*(6223), 1259855.

Stella, Battles, J. J., Orr, B. K., & McBride, J. R. (2006). Synchrony of seed dispersal, hydrology and local climate in a semi-arid river reach in california. *Ecosystems*, *9*(7), 1200–1214.

Stella, & Bendix, J. (2019). Multiple stressors in riparian ecosystems. In *Multiple stressors in river ecosystems* (pp. 81–110). Elsevier.

Stella, Vick, J., & Orr, B. (2003). Riparian vegetation dynamics on the merced river. In *California riparian systems: Processes and floodplains management, ecology,*

and restoration (2001 riparian habitat and floodplains conference proceedings), sacramento, ca (pp. 302–314).

Tron, S., Laio, F., & Ridolfi, L. (2014). Effect of water table fluctuations on phreatophytic root distribution. *Journal of Theoretical Biology*, *360*, 102–108.

Tron, S., Perona, P., Gorla, L., Schwarz, M., Laio, F., & Ridolfi, L. (2015). The signature of randomness in riparian plant root distributions. *Geophysical Research Letters*, *42*(17), 7098–7106.

Trush, W. J., McBain, S. M., & Leopold, L. B. (2000). Attributes of an alluvial river and their relation to water policy and management. *Proceedings of the National Academy of Sciences*, *97*(22), 11858–11863.

Tullos, D. D., Collins, M. J., Bellmore, J. R., Bountry, J. A., Connolly, P. J., Shafroth, P. B., & Wilcox, A. C. (2016). Synthesis of common management concerns associated with dam removal. *JAWRA Journal of the American Water Resources Association*, *52*(5), 1179–1206.

Tullos, D. D., Neumann, M., & Sanchez, J. J. A. (2004). Development of a qualitative model for investigating benthic community response to anthropogenic activities. *Proceedings of QR*, 2–4.

Tullos, D. D., Penrose, D. L., Jennings, G. D., & Cope, W. G. (2009). Analysis of functional traits in reconfigured channels: implications for the bioassessment and disturbance of river restoration. *Journal of the North American Benthological Society*, *28*(1), 80–92.

Uhlenbeck, G. E., & Ornstein, L. S. (1930). On the theory of the Brownian motion. *Physical review*, *36*(5), 823.

Wohl, E., Angermeier, P. L., Bledsoe, B., Kondolf, G. M., MacDonnell, L., Merritt, D. M., ... Tarboton, D. (2005). River restoration. *Water Resources Research*, *41*(10).

Wohl, E. E. (2004). *Disconnected rivers: linking rivers to landscapes*. Yale University Press.

Wong, M., & Parker, G. (2006). Reanalysis and Correction of Bed-Load Relation of Meyer-Peter and Müller Using Their Own Database. *Journal of Hydraulic Engineering*, *132*, 1159–1168.

Wu, W., & Wang, S. S. (2006). Formulas for sediment porosity and settling velocity. *Journal of Hydraulic Engineering*, *132*(8), 858–862.

Yang, S., Milliman, J., Xu, K., Deng, B., Zhang, X., & Luo, X. (2014). Downstream sedimentary and geomorphic impacts of the Three Gorges Dam on the Yangtze River. *Earth-Science Reviews*, *138*, 469–486.

Zahler, R. S., & Sussmann, H. J. (1977). Claims and accomplishments of applied catastrophe theory. *Nature*, *269*(5631), 759–763.